Synthetic and Structural Studies on Transition Metal Fullerene Complexes Containing Phosphorus and Arsenic Ligands: Crystal and Molecular Structures of (η^2-C_{60})M(dppf) (dppf = 1,1′-Bis(diphenylphosphino)ferrocene; M = Pt, Pd), (η^2-C_{60})Pt($AsPh_3$)$_2$, (η^2-C_{60})Pt(dpaf) (dpaf = 1,1′-Bis(diphenylarsino)ferrocene), and (η^2-C_{70})Pt(dpaf)

Li-Cheng Song,* Guan-Feng Wang, Peng-Chong Liu, and Qing-Mei Hu

Department of Chemistry, State Key Laboratory of Elemento-Organic Chemistry, Nankai University, Tianjin 300071, China

Received August 9, 2003

The reactions of C_{60} or C_{70} with $M(PPh_3)_4$ (M = Pt, Pd) in toluene or chlorobenzene at room temperature followed by in situ treatment of the intermediates (η^2-C_{60})$M(PPh_3)_2$ (**1**, M = Pt; **2**, M = Pd) or (η^2-C_{70})$M(PPh_3)_2$ (**3**, M = Pt; **4**, M = Pd) with dppf produced the corresponding bimetallic fullerene complexes (η^2-C_{60})M(dppf) (**5**, M = Pt; **6**, M = Pd) and (η^2-C_{70})M(dppf) (**7**, M = Pt; **8**, M = Pd). In addition, the reaction of C_{60} or C_{70} with $Pt(AsPh_3)_4$ and the reaction of C_{60} or C_{70} with $Pt(dba)_2$ (dba = dibenzylideneacetone) and $AsPh_3$ in toluene at room temperature both afforded the $AsPh_3$-containing fullerene complexes (η^2-C_{60})Pt-($AsPh_3$)$_2$ (**9**) and (η^2-C_{70})Pt($AsPh_3$)$_2$ (**10**), whereas both the reaction of the isolated **9** or **10** with diarsine ligand dpaf and the reaction of $Pt(AsPh_3)_4$ with C_{60} or C_{70} followed by in situ treatment of the intermediates **9** and **10** with dpaf in toluene at room temperature yielded the dpaf-containing bimetallic fullerene complexes (η^2-C_{60})Pt(dpaf) (**11**) and (η^2-C_{70})Pt(dpaf) (**12**).

Introduction

In view of the theoretical and practical importance of transition metal fullerene complexes,[1] a great variety of such complexes that contain single, double, triple, or multiple metal centers with various coordination patterns of the fullerene from η^1 to η^6 have been synthesized and structurally characterized.[2−5] However, among such reported metal complexes, no [60] and [70] fullerene complexes having arsenic ligands are known and very few such complexes containing dppf (1,1′-bis(diphenylphosphino)ferrocene) phosphorus ligands have been reported.[3h,5e] To further develop the synthetic and structural chemistry of transition metal fullerene complexes, we have prepared a series of new transition metal Pt/Pd fullerene complexes that contain the phosphorus and arsenic ligands $AsPh_3$, dppf, and dpaf (1,1′-bis(diphenylarsino)ferrocene). We report here the synthesis, characterization, and properties of fullerene complexes (η^2-C_{60})M(dppf) (**5**, M = Pt; **6**, M = Pd), (η^2-C_{70})M(dppf) (**7**, M = Pt; **8**, M = Pd), (η^2-C_{60})Pt($AsPh_3$)$_2$ (**9**), (η^2-C_{70})Pt($AsPh_3$)$_2$ (**10**), (η^2-C_{60})Pt(dpaf) (**11**), and (η^2-C_{70})Pt(dpaf) (**12**). The crystal structures of **5**, **6**, **9**, **11**, and **12** have been determined.

Results and Discussion

Synthesis and Spectroscopic Characterization of (η^2-C_{60})M(dppf) (5, M = Pt; 6, M = Pd) and (η^2-C_{70})M(dppf) (7, M = Pt; 8, M = Pd). A toluene solution of C_{60} or a chlorobenzene solution of C_{70} reacted with an equimolar quantity of $M(PPh_3)_4$ (M = Pt, Pd) at room temperature. Subsequent in situ treatment of the intermediate products, (η^2-C_{60})$M(PPh_3)_2$[6] and (η^2-C_{70})M-(PPh_3)$_2$,[7] with the diphosphine ligand dppf gave bimetallic fullerene complexes **5**−**8** in 65−86% yield (Scheme 1).

Complexes **5**−**8** are air-stable, dark green (for C_{60} derivatives **5** and **6**) or brown-red (for C_{70} derivatives **7** and **8**) solids, which are sparingly soluble in aromatic solvents such as toluene and chlorobenzene, but do not dissolve in nonpolar solvents such as hexane and petroleum ether.

* To whom correspondence should be addressed. Fax: 0086-22-23504853. E-mail: lcsong@public.tpt.tj.cn.

(1) See for example: (a) Fagan, P. J.; Calabrese, J. C.; Malone, B. *Acc. Chem. Res.* **1992**, *25*, 134. (b) Balch, A. L.; Olmstead, M. M. *Chem. Rev.* **1998**, *98*, 2123. (c) Lee, K.; Song, H.; Park, J. T. *Acc. Chem. Res.* **2003**, *36*, 78.

(2) For mononuclear fullerene derivatives, see: (a) Balch, A. L.; Catalano, V. J.; Lee, J. W.; Olmstead, M. M.; Parkin, S. R. *J. Am. Chem. Soc.* **1991**, *113*, 8953. (b) Balch, A. L.; Catalano, V. J.; Lee, J. W.; Olmstead, M. M. *J. Am. Chem. Soc.* **1992**, *114*, 5455. (c) Sawamura, M.; Iikura, H.; Nakamura, E. *J. Am. Chem. Soc.* **1996**, *118*, 12850. (d) Hsu, H.-F.; Du, Y.; Albrecht-Schmitt, T. E.; Wilson, S. R.; Shapley, J. R. *Organometallics* **1998**, *17*, 1756. (e) Song, L.-C.; Zhu, Y.-H.; Hu, Q.-M. *Polyhedron* **1997**, *16*, 2141. (f) Song, L.-C.; Zhu, Y.-H.; Hu, Q.-M. *Polyhedron* **1998**, *17*, 469. (g) Song, L.-C.; Zhu, Y.-H.; Hu, Q.-M. *J. Chem. Res., Synop.* **1999**, 56. (h) Song, L.-C.; Liu, J.-T.; Hu, Q.-M.; Weng, L.-H. *Organometallics* **2000**, *19*, 1643. (i) Thompson, D. M.; Bengough, M.; Baird, M. C. *Organometallics* **2002**, *21*, 4762. (j) Sawamura, M.; Kuninobu, Y.; Toganoh, M.; Matsuo, Y.; Yamanaka, M.; Nakamura, E. *J. Am. Chem. Soc.* **2002**, *124*, 9354. (k) Balch, A. L.; Costa, D. A.; Noll, B. C.; Olmstead, M. M. *Inorg. Chem.* **1996**, *35*, 458.

10.1021/om0341045 CCC: $25.00
Publication on Web 09/30/2003

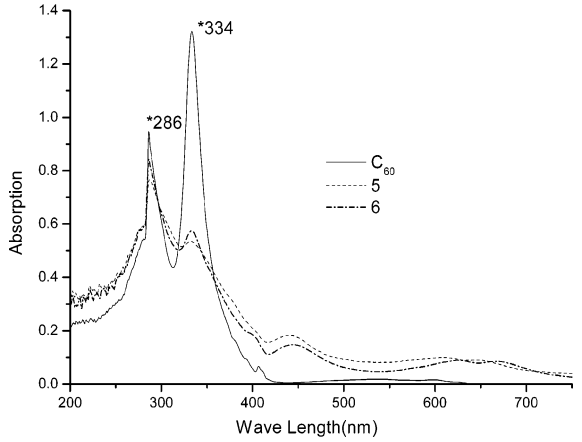

Figure 1. Comparison of the UV−vis spectra of C_{60}, **5**, and **6** in chlorobenzene at 290 K. *Data for C_{60}.

Scheme 1

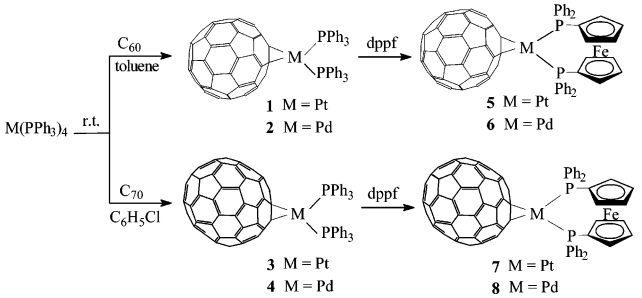

Figure 1 shows the UV−vis spectra of **5**, **6**, and C_{60}; Figure 2 displays those of **7**, **8**, and C_{70}. As can be seen from Figure 1, the absorption band at ca. 286 nm for **5** and **6** is almost identical with the corresponding band of free C_{60} in intensity. However, the absorption band at ca. 330 nm for **5** and **6** is much weaker than the corresponding band of free C_{60}. In addition, **5** and **6** all displayed a new absorption band at 439 or 444 nm, which can be considered as evidence for C_{60} being coordinated with Pt or Pd in an η^2-fashion through its 6:6 bond.[8]

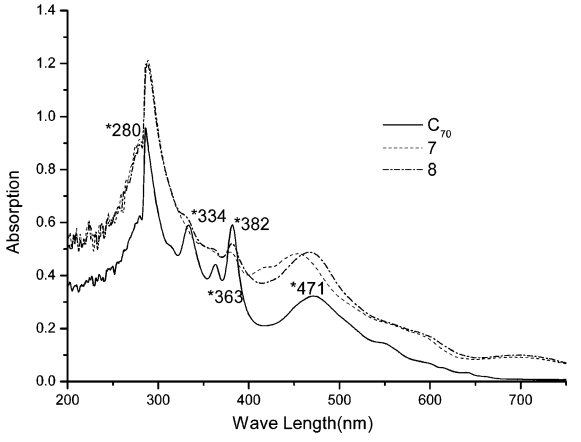

Figure 2. Comparison of the UV−vis spectra of C_{70}, **7**, and **8** in chlorobenzene at 290 K. *Data for C_{70}.

Similarly, in Figure 2 the absorption band at 289 nm for **7** or 288 nm for **8** is very close to the corresponding band of free C_{70} in intensity. However, the absorption bands at 334, 363, and 382 nm displayed by free C_{70} have completely disappeared or markedly weakened in the UV−vis spectra of **7** and **8**. These observations along with the much strengthened band at 455 or 467 nm for **7** and **8** as compared to the corresponding band of free C_{70} can be attributed to the C_{70} being coordinated to Pt or Pd in an η^2-fashion through its C_a−C_b 6:6 bond.[8]

Theoretical analyses indicated that the C_a−C_b 6:6 bonds at the poles of C_{70} are most reactive since they have higher π-bond order, a greatest degree of curvature at that site, and a degree of pyramidalization of the involved carbon atoms.[9,10] In addition, the X-ray diffraction analyses of the known C_{70} metal complexes, such as $(\eta^2\text{-}C_{70})Ir(CO)Cl(PPh_3)_2$,[2a] $(\eta^2\text{-}C_{70})Mo(CO)_3$-(dppe),[2d] and $(\eta^2\text{-}C_{70})Pd(PPh_3)_2$[7] have confirmed that all the transition metals are bound to C_{70} in an η^2-fashion through its C_a−C_b 6:6 bond. So, it is believed that **7** and **8** have the structures in which C_{70} is bonded to Pt or Pd through one of its C_a−C_b 6:6 bonds in an η^2-fashion. In fact, this is also consistent with the following observations: (i) **7** and **8** were produced simply by a ligand exchange reaction between $(\eta^2\text{-}C_{70})M(PPh_3)_2$ and dppf, which does not involve breaking of the bonding between C_a−C_b and Pt or Pd in the starting materials $(\eta^2\text{-}C_{70})M(PPh_3)_2$; (ii) the As analogue of **7**, i.e., $(\eta^2\text{-}C_{70})$-Pt(dpaf), synthesized by the same type of reaction has been confirmed by X-ray diffraction analysis to have the Pt atom bound to the C_a−C_b bond of C_{70} in an η^2-fashion (vide infra). In addition, although the molecules of **7** and **8** are unsymmetrical, the two different P atoms in dppf of each molecule displayed only one singlet respectively at 13.28 and 34.06 ppm, probably due to the bond rotation between C_{70} and Pt or Pd in solution.

So far, the Mössbauer behavior of the iron-containing fullerene complexes remained unknown. To see the influence of the fullerene moiety upon the Mössbauer behavior of the iron-containing unit, we determined the first ^{57}Fe Mössbauer spectrum of the iron-containing fullerene compound **5**. For comparison, however, we also determined the Mössbauer spectrum of the dppf ligand.

(3) For dinuclear fullerene derivatives, see: (a) Balch, A. L.; Lee, J. W.; Noll, B. C.; Olmstead, M. M. *J. Am. Chem. Soc.* **1992**, *114*, 10984. (b) Balch, A. L.; Lee, J. W.; Olmstead, M. M. *Angew. Chem., Int. Ed. Engl.* **1992**, *31*, 1356. (c) Zhang, S.; Brown, T. L.; Du, Y.; Shapley, J. R. *J. Am. Chem. Soc.* **1993**, *115*, 6705. (d) Balch, A. L.; Lee, J. W.; Noll, B. C.; Olmstead, M. M. *Inorg. Chem.* **1994**, *33*, 5238. (e) Mavunkal, I. J.; Chi, Y.; Peng, S.-M.; Lee, G.-H. *Organometallics* **1995**, *14*, 4454. (f) Zhu, Y.-H.; Song, L.-C.; Hu, Q.-H.; Li, C.-M. *Org. Lett.* **1999**, *1*, 1693. (g) Song, L.-C.; Zhu, Y.-H.; Hu, Q.-M. *J. Chem. Res., Synop.* **2000**, 316. (h) Song, L.-C.; Liu, J.-T.; Hu, Q.-M.; Wang, G.-F.; Zanello, P.; Fontani, M. *Organometallics* **2000**, *19*, 5342. (i) Song, L.-C.; Liu, J.-T.; Hu, Q.-M. *J. Organomet. Chem.* **2002**, *662*, 51.

(4) For trinuclear fullerene derivatives, see: (a) Hsu, H.-F.; Shapley, J. R. *J. Am. Chem. Soc.* **1996**, *118*, 9192. (b) Hsu, H.-F.; Shapley, J. R. *J. Chem. Soc., Chem. Commun.* **1997**, 1125. (c) Song, H.; Lee, K.; Park, J. T.; Choi, M.-G. *Organometallics* **1998**, *17*, 4477. (d) Song, H.; Choi, J. I.; Lee, K.; Choi, M.-G.; Park, J. T. *Organometallics* **2002**, *21*, 5221.

(5) For multinuclear fullerene derivatives, see: (a) Fagan, P. J.; Calabrese, J. C.; Malone, B. *J. Am. Chem. Soc.* **1991**, *113*, 9408. (b) Rasinkangas, M.; Pakkaned, T. T.; Pakkaned, T. A.; Ahlgrén, M.; Rouvinen, J. *J. Am. Chem. Soc.* **1993**, *115*, 4901. (c) Balch, A. L.; Hao, L.; Olmstead, M. M. *Angew. Chem., Int. Ed. Engl.* **1996**, *35*, 188. (d) Lee, K.; Hsu, H.-F.; Shapley, J. R. *Organometallics* **1997**, *16*, 3876. (e) Lee, K.; Shapley, J. R. *Organometallics* **1998**, *17*, 3020. (f) Hsu, H.-F.; Wilson, S. R.; Shapley, J. R. *J. Chem. Soc., Chem. Commun.* **1997**, 1125.

(6) (a) Lerke, S. A.; Parkinson, B. A.; Evans, D. H.; Fagan, P. J. *J. Am. Chem. Soc.* **1992**, *114*, 7807. (b) Bashilov, V. V.; Petrovskii, P. V.; Sokolov, V. I.; Lindeman, S. V.; Guzey, I. A.; Struchkov, Y. T. *Organometallics* **1993**, *12*, 991.

(7) Olmstead, M. M.; Hao, L.; Balch, A. L. *J. Organomet. Chem.* **1999**, *578*, 85.

(8) Chernega, A. N.; Green, L. H.; Haggitt, J.; Stephen, A. H. H. *J. Chem. Soc., Dalton Trans.* **1998**, 755.

(9) Taylor, R. *J. Chem. Soc., Perkin Trans. 2* **1993**, 813.

(10) Haddon, R. C. *Science* **1993**, *261*, 1545.

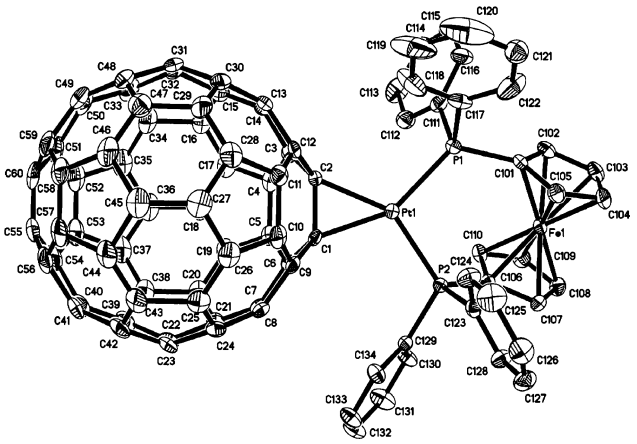

Figure 3. Molecular structure of **5**.

Table 1. Selected Bond Lengths (Å) and Angles (deg) for 5 and 6

		5	
Pt(1)−C(1)	2.088(5)	P(1)−C(111)	1.822(6)
Pt(1)−C(2)	2.140(5)	Pt(1)−P(2)	2.2700(13)
Pt(1)−P(1)	2.2980(14)	C(1)−C(2)	1.513(7)
C(1)−Pt(1)−C(2)	41.90(19)	C(111)−P(1)−C(117)	103.7(3)
P(1)−Pt(1)−P(2)	102.96(5)	C(117)−P(1)−C(101)	102.7(3)
C(1)−Pt(1)−P(2)	104.45(14)	C(2)−Pt(1)−P(1)	110.69(14)
		6	
Pd(1)−C(1)	2.087(9)	P(1)−C(111)	1.789(10)
Pd(1)−C(2)	2.120(9)	Pd(1)−P(2)	2.286(3)
Pd(1)−P(1)	2.331(3)	C(1)−C(2)	1.466(11)
C(1)−Pd(1)−C(2)	40.8(3)	C(111)−P(1)−C(117)	103.4(4)
P(1)−Pd(1)−P(2)	103.30(9)	C(117)−P(1)−C(101)	102.7(4)
C(1)−Pd(1)−P(2)	104.4(2)	C(2)−Pd(1)−P(1)	111.6(2)

The two spectra are very similar in shape, both displaying a doublet with an equal intensity. The isomeric shift (IS) value (0.39 mm/s) of **5** is slightly less than that (0.43 mm/s) of dppf, as expected since C_{60} is a weak electron-accepting ligand and the IS value is proportional to the change in the electron density at the iron nucleus.[11] In addition, since the quadruple splitting (QS) value (2.24 mm/s) of **5** and that (2.30 mm/s) of dppf are very similar, the symmetry of the electron cloud around the octahedral Fe atom in each of these compounds appears to be very similar.[12]

Crystal Structures of 5 and 6. The crystal structures of **5** and **6** have been unequivocally confirmed by X-ray diffraction studies, which are actually isostructural. While Figure 3 shows the molecular structure of **5** (for **6**, see the Supporting Information), Table 1 lists their selected bond lengths and angles. The ferrocene-containing diphosphine dppf ligand chelates the Pt or Pd atom, while the C_{60} cage coordinates to Pt or Pd in an η^2-fashion via its C(1)−C(2) bond between two six-membered rings. The atoms C(1), C(2), P(1), P(2) and Pt(1) or Pd(1) for **5** and **6** are almost coplanar with a mean deviation of 0.0025 Å for **5** and 0.0056 Å for **6**. In the Pt(1) or Pd(1)−C(1)−C(2) heterocyclopropane moiety, the C(1)−C(2) bond length (1.513(7) Å for **5** and 1.466(11) Å for **6**) is very close to the corresponding values observed in $(\eta^2\text{-}C_{60})Pt(PPh_3)_2$ (1.50(3) Å)[13] and $(\eta^2\text{-}C_{60})Pd(PPh_3)_2$ (1.45(3) Å),[6b] which are considerably longer than that of free C_{60} (1.38 Å)[14] due to metal-to-C_{60} π-back-donation.[3a] It might be suggested that the π-back-donation in **5** is stronger than that in **6** since the C(1)−C(2) bond length in **5** is longer than that in **6**.

Table 2. Comparison of the Crystal Structure and Optimized Structure of 6

structural parameter		crystal structure	optimized structure
distance (Å)	Pd···Fe	4.196	2.616
bond length (Å)	C(1)−C(2)	1.466(11)	1.365
	Pd(1)−C(1)	2.087(9)	2.135
	Pd(1)−P(2)	2.286(3)	2.334
bond angle (deg)	C(1)−Pd(1)−C(2)	40.8(3)	37.3
	C(1)−Pd(1)−P(2)	104.4(2)	156.2
	C(2)−Pd(1)−P(1)	111.6(2)	156.2

Complex **6** was previously prepared by Bashilov and co-workers,[15] but they did not determine its molecular structure by X-ray diffraction techniques. Instead, they reported its optimized structure as obtained by the molecular mechanics MM+ method.[15] This "optimized" structure of **6** deviates severely from the "real" structure of **6** as determined by X-ray diffraction. This can be seen by comparing some of their structural parameters compiled in Table 2. For example, (i) the bond angles of C(1)−Pd(1)−P(2) (104.4(2)°) and C(2)−Pd(1)−P(1) (111.6(2)°) confirmed by X-ray diffraction analysis are consiberably smaller than the corresponding angles (156.2°) in the optimized structure, and (ii) the Pd−Fe distance confirmed by X-ray diffraction analysis is 4.196 Å, which is much longer than that (2.616 Å) in the optimized structure. Such a large distance between Pd and Fe is far greater than the sum of their van der Waals radii and thus far beyond the range of a Pd−Fe metal−metal interaction. It follows that the overlapping of the orbitals of Pd and Fe in **6** suggested by Bashilov and co-workers[15] is not correct. Furthermore, the ferrocene structural moiety in the optimized structure is bent,[15] whereas the X-ray diffraction analysis of **6** shows that the two substituted Cp rings (dihedral angle = 2.3°) in the ferrocene moiety are basically parallel and arranged in a staggered manner.

Synthesis and Spectroscopic Characterization of $(\eta^2\text{-}C_{60})Pt(AsPh_3)_2$ (9), $(\eta^2\text{-}C_{70})Pt(AsPh_3)_2$ (10), $(\eta^2\text{-}C_{60})Pt(dpaf)$ (11), and $(\eta^2\text{-}C_{70})Pt(dpaf)$ (12). The reaction of an equimolar amount of $Pt(AsPh_3)_4$ with C_{60} or C_{70} and the reaction of an equimolar amount of $Pt(dba)_2$ (dba = dibenzylideneacetone) with C_{60} or C_{70} in the presence of an excess of $AsPh_3$ in toluene at room temperature produced the $AsPh_3$-containing fullerene complexes **9** and **10** in 61−81% yield (Scheme 2).

In addition, the diarsine dpaf-containing bimetallic fullerene complexes **11** and **12** were prepared both by the reaction of the isolated **9** or **10** with an equimolar quantity of dpaf and by the reaction of $Pt(AsPh_3)_4$ with an equimolar quantity of C_{60} or C_{70} followed by in situ treatment of the intermediate products **9** and **10** with

(11) Burger, K.; Korecz, L.; Bor, G. J. *Inorg. Nucl. Chem.* **1969**, *31*, 1527.

(12) (a) Cooke, C. G.; Mays, M. J. *J. Chem. Soc., Dalton Trans.* **1975**, 455. (b) Zhang, J.-K.; Song, L.-C.; Zhang, Z.-M.; Liu, R.-G.; Cheng, Z.-Z.; Wang, J.-T. *Hyperfine Interact.* **1988**, *40*, 363.

(13) Fagan, P. J.; Calabrese, J. C.; Malone, B. *Science* **1991**, *252*, 1160.

(14) Bürgi, H. B.; Blanc, E.; Schwarzenbach, D.; Liu, S.; Lu, Y.; Kappes, M. M.; Ibers, J. A. *Angew. Chem., Int. Ed. Engl.* **1992**, *31*, 640.

(15) Bashilov, V. V.; Magdesieva, T. V.; Kravchuk, D. N.; Petrovskii, P. V.; Ginzburg, A. G.; Butin, K. P.; Sokolov, V. I. *J. Organomet. Chem.* **2000**, *599*, 37.

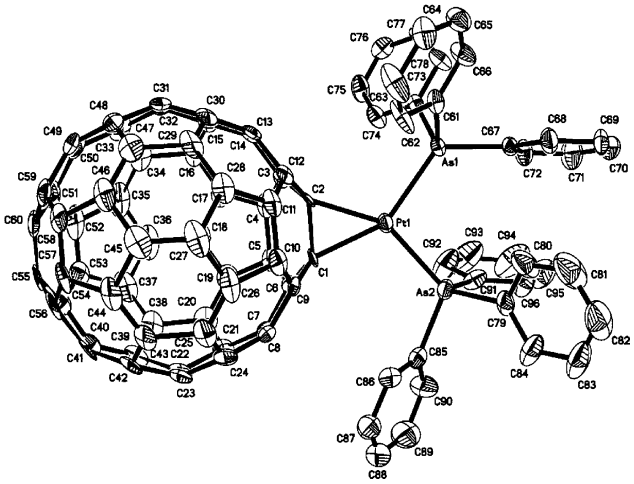

Figure 4. Molecular structure of **9**.

Scheme 2

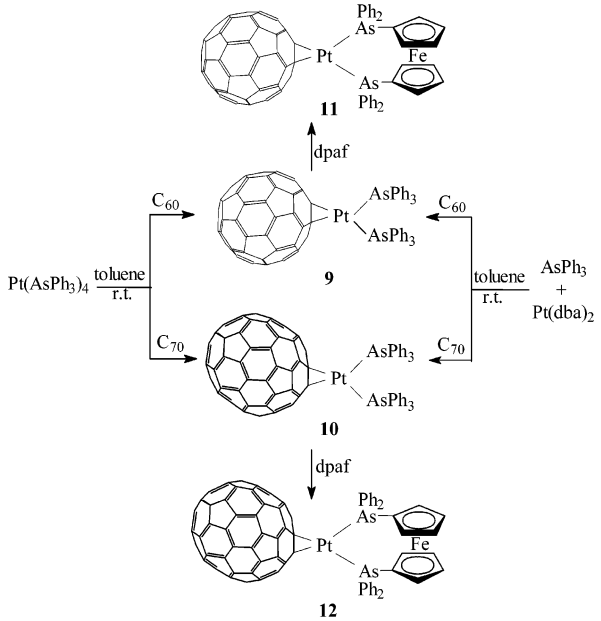

dpaf in toluene at room temperature in 67−85% yield (Scheme 2). The latter route to **11** and **12** is much more convenient than the former one since it involves a sequential "one-pot" reaction without isolation of **9** and **10**.

Products **9**−**12** are the first examples of transition metal C_{60} and C_{70} fullerene complexes containing arsenic ligands, although the fullerene oxide ($C_{60}O$) iridium complex with $AsPh_3$ was previously reported.[2k] Compounds **9**−**12** are air-stable and dark green (for **9** and **11**) or brown-red (for **10** and **12**) solids. They are very similar to the phosphorus compounds **1**−**8** and have been fully characterized by elemental analysis, spectroscopy, and X-ray diffraction analyses.

Crystal Structures of 9, 11, and 12. The structures of **9**, **11**, and **12** have been unambiguously confirmed by X-ray crystallography. Figures 4 and 5 present the molecular structures of **9** and **12** (for **11**, see the Supporting Information), whereas Table 3 lists their selected bond lengths and angles. Figure 4 shows that complex **9** indeed consists of two $AsPh_3$ and one C_{60} ligand all coordinated to the central Pt(1) atom through As(1) and As(2), as well as the C(1)−C(2) 6:6 bond. The

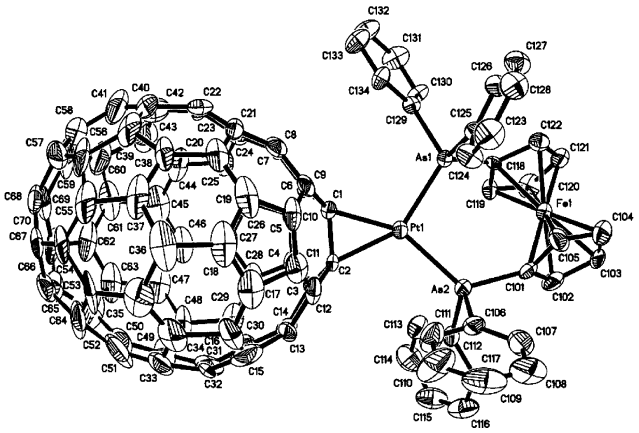

Figure 5. Molecular structure of **12**.

Table 3. Selected Bond Lengths (Å) and Angles (deg) for 9, 11, and 12

		9	
Pt(1)−C(1)	2.113(8)	C(1)−C(2)	1.513(13)
Pt(1)−C(2)	2.108(9)	As(1)−C(67)	1.938(10)
Pt(1)−As(1)	2.4312(13)	Pt(1)−As(2)	2.3890(16)
C(1)−Pt(1)−C(2)	42.0(3)	C(73)−As(1)−C(67)	98.7(4)
As(1)−Pt(1)−As(2)	102.31(5)	C(73)−As(1)−C(61)	104.4(4)
C(1)−Pt(1)−As(2)	107.5(3)	C(2)−Pt(1)−As(1)	108.2(2)
		11	
Pt(1)−C(1)	2.083(7)	As(1)−C(111)	1.953(8)
Pt(1)−C(2)	2.119(7)	C(1)−C(2)	1.518(10)
Pt(1)−As(1)	2.4083(10)	Pt(1)−As(2)	2.3874(9)
C(1)−Pt(1)−C(2)	42.3(3)	C(101)−As(1)−Pt(1)	122.1(2)
As(1)−Pt(1)−As(2)	100.12(3)	C(111)−As(1)−C(117)	104.5(4)
C(1)−Pt(1)−As(2)	105.79(19)	C(2)−Pt(1)−As(1)	111.8(2)
		12	
Pt(1)−C(1)	2.072(10)	As(1)−C(112)	1.936(12)
Pt(1)−C(2)	2.101(10)	C(1)−C(2)	1.480(13)
Pt(1)−As(1)	2.3971(17)	Pt(1)−As(2)	2.3786(15)
C(1)−Pt(1)−C(2)	41.5(4)	C(101)−As(1)−Pt(1)	122.2(3)
As(1)−Pt(1)−As(2)	100.61(5)	C(101)−As(1)−C(112)	102.3(5)
C(1)−Pt(1)−As(2)	106.6(3)	C(2)−Pt(1)−As(1)	111.3(3)

Pt(1), As(1), As(2), C(1), and C(2) atoms are coplanar with deviations from the least-squares plane within 0.046 Å. The bond angles of C(1)−Pt(1)−C(2) (42.0(3)°) and As(1)−Pt(1)−As(2) (102.31(5)°) are almost identical with the corresponding ones in (η^2-C_{60})$Pt(PPh_3)_2$ (41.3(8)° and 102.4(2)°, respectively).[13] However, the average bond length of Pt−As in **9** (2.4101(14) Å) is much longer than that of Pt−P in (η^2-C_{60})$Pt(PPh_3)_2$ (2.278(7) Å),[13] which is in agreement with the 0.13 Å difference in the covalent bond radii of As (1.21 Å) and P (1.10 Å).[16]

Complex **12** contains one dpaf ligand chelated to Pt(1) through As(1) and As(2) and one C_{70} ligand coordinated to Pt(1) through one of its 10 C_a−C_b 6:6 bonds, namely, the C(1)−C(2) 6:6 bond. The two cyclopentadienyl rings in dpaf ligand are almost parallel with a dihedral angle of only 1.3°. There are no metal−metal interactions between Pt(1) and Fe(1) since the distance between Pt(1) and Fe(1) (4.4186 Å) is well beyond their van der Waals contacts. In addition, it is due to the π-back-donation between Pt atom and the C_a−C_b 6:6 bond in coordinated C_{70} that the C(1)−C(2) bond is slightly elongated to 1.480(13) Å from the original 1.468 Å in

(16) Pauling, L. *The Nature of the Chemical Bond*; Cornell University Press: Ithaca, New York, 1967.

free C_{70}.[17] Finally, it should be noted that one unit cell of **11** or **12** contains four molecules of **11** or **12** and two molecules of solvent toluene. There are no appreciable interactions of the fullerene moiety in **11** or **12** with the solvent molecule toluene since the nearest distance between them is ca. 3.7 Å, far beyond the van der Waals contacts.

Experimental Section

General Comments. All reactions were carried out under highly purified nitrogen atmosphere using standard Schlenk or vacuum-line techniques. Toluene was distilled from Na/benzophenone ketyl, while chlorobenzene was dried over P_2O_5 and distilled from CaH_2. Other solvents were bubbled with nitrogen for at least 15 min before use. $Pt(PPh_3)_4$,[18] $Pd(PPh_3)_4$,[19] $Pt(AsPh_3)_4$,[18] $Pt(dba)_2$,[20] dppf,[20] and dpaf[21] were prepared according to literature methods. C_{60} (99.9%) and C_{70} (99.9%) were available commercially. ^{1}H NMR spectra were recorded on a Bruker AC P200 or a Mercury VX (Varian)-300 spectrometer, while UV−vis and IR spectra were taken on Shimadzu UV 240 and Bio-Rad FTS 135 spectrophotometers, respectively. Elemental analysis was performed on an Elementar Vario EL analyzer. The Mössbauer spectra were recorded on a MS-500 Mössbauer spectrometer using ^{57}Co diffused in a Pd matrix as radiation source. The isomeric shifts were recorded relative to natural iron foil at 293 K. Melting points were determined on a Yanaco MP-500 apparatus.

Preparation of (η^2-C_{60})Pt(dppf) (5). A 100 mL three-necked flask equipped with a magnetic stir-bar, a rubber septum, and a nitrogen inlet tube was charged with 54 mg (0.075 mmol) of C_{60}, 20 mL of toluene, and 94 mg (0.075 mmol) of $Pt(PPh_3)_4$. The mixture was stirred at room temperature for 0.5 h to give a dark green solution containing (η^2-C_{60})Pt-$(PPh_3)_2$. To this solution was added 42 mg (0.075 mmol) of dppf, and stirring continued for another 0.5 h. Then, this new mixture was carefully layered with 60 mL of hexane. After standing overnight, the mixture was filtered to give a precipitate, which was washed with 15 mL of toluene and 10 mL of pentane and dried in vacuo, resulting in 72 mg (65%) of **5** as a dark green solid, mp > 300 °C. Anal. Calcd for $C_{94}H_{28}FeP_2$-Pt: C 76.80, H 1.92. Found: C 76.65, H 2.05. IR (KBr disk): $\nu_{C_{60}}$ 1434 (s), 1185 (m), 577 (m), 525 (vs) cm^{-1}. ^{1}H NMR ($CDCl_3$, TMS): δ 4.17 (s, 4H, 2H^3, 2H^4), 4.34 (s, 4H, 2H^2, 2H^5), 7.24−7.90 (m, 20H, 4C_6H_5) ppm. UV−vis (PhCl): λ_{max} (log ϵ) 286 (4.72), 332 (4.57), 439 (4.10) nm.

Preparation of (η^2-C_{60})Pd(dppf) (6). Similarly, when 87 mg (0.075 mmol) of $Pd(PPh_3)_4$ was utilized instead of $Pt(PPh_3)_4$, 71 mg (69%) of **6** as a dark green solid was obtained, mp > 300 °C. Anal. Calcd for $C_{94}H_{28}FeP_2Pd$: C 81.73, H 2.04. Found: C 81.99, H 2.25. IR (KBr disk): $\nu_{C_{60}}$ 1434 (s), 1184 (m), 578 (m), 526 (s) cm^{-1}. ^{1}H NMR ($CDCl_3$, TMS): δ 4.20 (s, 4H, 2H^3, 2H^4), 4.39(s, 4H, 2H^2, 2H^5), 7.13−7.90 (m, 20H, 4 C_6H_5) ppm. UV−vis (PhCl): λ_{max} (log ϵ) 286 (4.72), 333 (4.55), 444 (3.96) nm.

Preparation of (η^2-C_{70})Pt(dppf) (7). The flask described above was charged with 21 mg (0.025 mmol) of C_{70}, 15 mL of chlorobenzene, and 32 mg (0.025 mmol) of $Pt(PPh_3)_4$. The reaction mixture was stirred at room temperature for 1 h to produce a brown-red solution containing (η^2-C_{70})$Pt(PPh_3)_2$. To this solution was added 25 mg (0.045 mmol) of dppf, and stirring continued for an additional 0.5 h to give a new mixture, which was layered with 60 mL of petroleum ether. After standing overnight, the mixture was filtered and the brown precipitate was washed with 4 mL of pentane and dried in vacuo, producing 34 mg (86%) of **7** as a brown-red solid, mp > 300 °C. Anal. Calcd for $C_{104}H_{28}FeP_2Pt$: C 78.55, H 1.77. Found: C 78.60, H 1.68. IR (KBr disk): $\nu_{C_{70}}$ 1479 (m), 1432 (vs), 1125 (w), 1095 (m), 794 (w), 673 (m), 576 (m), 534 (s) cm^{-1}. ^{1}H NMR ($CDCl_3$, TMS): δ 4.16 (s, 4H, 2H^3, 2H^4), 4.34 (s, 4H, 2H^2, 2H^5), 7.05−8.94 (m, 20H, 4 C_6H_5) ppm. ^{31}P NMR ($CDCl_3$, H_3PO_4): δ 13.28 (s, 2P) ppm. UV−vis (PhCl): λ_{max} (log ϵ) 289 (4.81), 379 (4.42), 455 (4.40) nm. MS (FAB): *m*/*z* 1590 (M$^+$, ^{195}Pt).

Preparation of (η^2-C_{70})Pd(dppf) (8). Similarly, when 30 mg (0.025 mmol) of $Pd(PPh_3)_4$ was used instead of $Pt(PPh_3)_4$, 26 mg (69%) of **8** as a brown-red solid was obtained, mp > 300 °C. Anal. Calcd for $C_{104}H_{28}FeP_2Pd$: C 83.19, H 1.88. Found: C 83.12, H 2.00. IR (KBr disk): $\nu_{C_{70}}$ 1478 (m), 1431 (s), 1094 (m), 794 (m), 673 (m), 577 (m), 535 (s), 461 (s) cm^{-1}. ^{1}H NMR ($CDCl_3$, TMS): δ 4.17 (s, 4H, 2H^3, 2H^4), 4.37 (s, 4H, 2H^2, 2H^5), 7.05−8.94 (m, 20H, 4 C_6H_5) ppm. ^{31}P NMR ($CDCl_3$, H_3PO_4): δ 34.06 (s, 2P) ppm. UV−vis (PhCl): λ_{max} (log ϵ) 288 (4.79), 382 (4.43), 467 (4.40) nm. MS (FAB): *m*/*z* 1503 (M$^+$, ^{108}Pd).

Preparation of (η^2-C_{60})$Pt(AsPh_3)_2$ (9). Method (i). The flask described above was charged with 18 mg (0.025 mmol) of C_{60}, 10 mL of toluene, and 36 mg (0.025 mmol) of $Pt(AsPh_3)_4$. The mixture was stirred at room temperature for 0.5 h, and then onto the mixture was carefully placed a layer of 15 mL of hexane. The system was allowed to stand overnight to give a dark green precipitate, which was fillered, washed with 15 mL of hexane, and dried in vacuo to afford 31 mg (81%) of **9** as a dark green solid, mp > 300 °C. Anal. Calcd for $C_{96}H_{30}$-As_2Pt: C, 75.45; H, 1.98. Found: C, 75.17; H, 1.96. IR (KBr disk): $\nu_{C_{60}}$ 1434 (s), 1184 (s), 579 (m), 526 (vs) cm^{-1}. ^{1}H NMR ($CDCl_3$): δ 7.11−7.72 (m, 30H, 6 C_6H_5) ppm. UV−vis (PhCl): λ_{max} (log ϵ) 287 (4.76), 333 (4.71), 425 (3.90) nm.

Method (ii). The flask described above was charged with 18 mg (0.025 mmol) of C_{60}, 10 mL of toluene, 17 mg (0.025 mmol) of $Pt(dba)_2$, and 24 mg (0.075 mmol) of $AsPh_3$. The mixture was stirred at room temperature for 0.5 h, and then onto this solution was carefully placed a layer of 15 mL of hexane. The two-layer system was allowed to stand overnight to give a dark green precipitate. The same workup as that in method (i) afforded 29 mg (76%) of **9**.

Preparation of (η^2-C_{70})$Pt(AsPh_3)_2$ (10). Method (i). The same procedure as method (i) for the preparation of **9** was followed, but 21 mg (0.025 mmol) of C_{70} was used instead of C_{60} to give 30 mg (73%) of **10** as a brown-red solid, mp > 300 °C. Anal. Calcd for $C_{106}H_{30}As_2Pt$: C, 77.24; H, 1.83. Found: C, 77.35; H, 2.03. IR (KBr disk): $\nu_{C_{70}}$ 1433 (vs), 1414 (w), 1087 (m), 1079 (m), 794 (m), 673 (s), 640 (s), 578 (s), 533 (s), 471 (s), 457 (s) cm^{-1}. ^{1}H NMR ($CDCl_3$): δ 7.13−7.72 (m, 30 H, 6C_6H_5) ppm. UV−vis (PhCl): λ_{max} (log ϵ) 287 (4.94), 332 (4.66), 363 (4.54), 382 (4.62), 464 (4.46), 554 (4.16) nm.

Method (ii). The same procedure as method (ii) for the preparation of **9** was followed, but 21 mg (0.025 mmol) of C_{70} was utilized instead of C_{60} to yield 25 mg (61%) of **10**.

Preparation of (η^2-C_{60})Pt(dpaf) (11). Method (i). The flask described above was charged with 18 mg (0.025 mmol) of C_{60}, 10 mL of toluene, and 36 mg (0.025 mmol) of $Pt(AsPh_3)_4$. The mixture was stirred at room temperature for 0.5 h, and then 16 mg (0.025 mmol) of dpaf was added. The new mixture was stirred continuously for 0.5 h to give a dark green solution. Then, onto this solution was carefully placed a layer of 15 mL of hexane. The two-layer system was allowed to stand overnight to give a dark green precipitate. The precipitate was filtered, washed with 15 mL of toluene and 10 mL of hexane, and dried in vacuo to afford 27 mg (70%) of **11** as a dark green solid, mp > 300 °C. Anal. Calcd for $C_{94}H_{28}As_2FePt$: C, 72.47; H, 1.81. Found: C, 72.23; H, 1.67. IR (KBr disk): $\nu_{C_{60}}$ 1434 (s), 1184 (s), 577 (s), 548 (s) cm^{-1}. ^{1}H NMR ($CDCl_3$): δ 4.05 (s, 4H,

(17) Negri, F.; Orlandi, G.; Zerbetto, F. *J. Am. Chem. Soc.* **1991**, *113*, 6037.
(18) Malatesta, L.; Variello, C. *J. Chem. Soc.* **1958**, 2323.
(19) Malatesta, L.; Angoletta, M. *J. Chem. Soc.* **1957**, 1186.
(20) Bishop, J. J.; Davison, A.; Katcher, M. L.; Lichtenberg, D. M.; Merril, R. E.; Smart, J. C. *J. Organomet. Chem.* **1971**, *27*, 241.
(21) Das, M.; Livingstone, S. E.; Filipczuk, S. W.; Hayes, J. W.; Radford, D. V. *J. Chem. Soc., Dalton Trans.* **1974**, 1409.

$2H^3$, $2H^4$), 4.27 (s, 4H, $2H^2$, $2H^5$), 7.10−7.82 (m, 20H, $4C_6H_5$) ppm. UV−vis (PhCl): λ_{max} (log ϵ) 286 (4.73), 333 (4.76), 465 (4.15) nm.

Method (ii). The flask described above was charged with 19 mg (0.0125 mmol) of **9**, 10 mL of toluene, and 8 mg (0.0125 mmol) of dpaf. The mixture was stirred at room temperature for 0.5 h to give a dark green solution. Then, this solution was carefully layered with 10 mL of hexane. The two-layer system was allowed to stand overnight to give a precipitate. The same workup as that in method (i) afforded 13 mg (67%) of **11**.

Preparation of (η^2-C_{70})Pt(dpaf) (12). Method (i). The same procedure as method (i) for the preparation of **11** was followed, but 21 mg (0.025 mmol) of C_{70} was employed instead of C_{60} to afford 36 mg (85%) of **12** as a brown-red solid, mp > 300 °C. Anal. Calcd for $C_{104}H_{28}As_2FePt$: C, 74.44; H, 1.68. Found: C, 74.42; H, 1.60. IR (KBr disk): $\nu_{C_{70}}$ 1432 (vs), 1126 (s), 1080 (s), 1025 (s), 820 (s), 794 (s), 673 (s), 640 (m), 577 (s), 460 (vs) cm^{-1}. ^1H NMR ($CDCl_3$): δ 4.05 (s, 4H, $2H^3$, $2H^4$), 4.27 (s, 4H, $2H^2$, $2H^5$), 7.10−7.74 (m, 20H, $4C_6H_5$) ppm. UV−vis (PhCl): λ_{max} (log ϵ) 286 (4.74), 333 (4.49), 363 (4.37), 382 (4.47), 464 (4.25) nm.

Method (ii). The same procedure as method (ii) for the preparation of **11** was followed, but 21 mg (0.0125 mmol) of **10** was used instead of **9** to give 17 mg (81%) of **12**.

X-ray Crystal Structure Determinations of 5, 6, 9, 11, and 12. Single crystals of **5**·0.5PhCl, **6**·0.5PhCl, **9**, **11**·0.5PhMe, and **12**·0.5PhMe suitable for X-ray diffraction studies were obtained by various interlayer diffusion methods (see the Supporting Information). Each single crystal was glued to a glass fiber and mounted on a Bruker SMART 1000 automated diffractometer, respectively. Data were collected at room temperature, using Mo Kα graphite-monochromated radiation (λ = 0.71073 Å) in the ω−2θ scanning mode. Absorption corrections were performed using SADABS. The structures were solved by direct methods using the SHELXTL-97 program and refined by full-matrix least-squares techniques (SHELXL-97) on F^2. Hydrogen atoms were located by using the geometric method. All calculations were performed on a Bruker Smart computer.

Acknowledgment. We are grateful to the National Natural Science Foundation of China and the Special Fund for Doctoral Program from the Ministry of China for financial support of this work.

Supporting Information Available: Crystal growing procedures and full tables of crystal data, atomic coordinates and thermal parameters, and bond lengths and angles for **5**, **6**, **9**, **11**, and **12**; ORTEP drawings of **6** and **11**; molecular arrangement in an unit cell of **5**, **6**, **11**, and **12**; and a ^{57}Fe Mössbauer spectrum of **5**. This material is available free of charge via the Internet at http://pubs.acs.org.

OM0341045